



# Prophage Excision in *Streptococcus pneumoniae* Serotype 19A ST320 Promote Colonization: Insight Into Its Evolution From the Ancestral Clone Taiwan 19F-14 (ST236)

Yi-Yin Chen<sup>1†</sup>, Jin-Town Wang<sup>2,3†</sup>, Tzu-Lung Lin<sup>4</sup>, Yu-Nong Gong<sup>5</sup>, Ting-Hsuan Li<sup>1</sup>, Ya-Yu Huang<sup>1</sup> and Yu-Chia Hsieh<sup>1\*</sup>

## OPEN ACCESS

### Edited by:

Leonard Peruski,  
Centers for Disease Control  
and Prevention (CDC), United States

### Reviewed by:

Adela González De La Campa,  
Instituto de Salud Carlos III, Spain  
Hajjian Zhou,  
National Institute for Communicable  
Disease Control and Prevention  
(China CDC), China

### \*Correspondence:

Yu-Chia Hsieh  
yuchiahsieh@gmail.com

<sup>†</sup>These authors have contributed  
equally to this work

### Specialty section:

This article was submitted to  
Infectious Diseases,  
a section of the journal  
Frontiers in Microbiology

Received: 31 July 2018

Accepted: 24 January 2019

Published: 08 February 2019

### Citation:

Chen Y-Y, Wang J-T, Lin T-L,  
Gong Y-N, Li T-H, Huang Y-Y and  
Hsieh Y-C (2019) Prophage Excision  
in *Streptococcus pneumoniae*  
Serotype 19A ST320 Promote  
Colonization: Insight Into Its Evolution  
From the Ancestral Clone Taiwan  
19F-14 (ST236).  
Front. Microbiol. 10:205.  
doi: 10.3389/fmicb.2019.00205

<sup>1</sup> Department of Pediatrics, Chang Gung Children's Hospital, Chang Gung Memorial Hospital, College of Medicine, Chang Gung University, Taoyuan, Taiwan, <sup>2</sup> Department of Microbiology, National Taiwan University College of Medicine, Taipei, Taiwan, <sup>3</sup> Department of Internal Medicine, National Taiwan University Hospital, Taipei, Taiwan, <sup>4</sup> Department of Medical Biotechnology and Laboratory Science, College of Medicine, Chang Gung University, Taoyuan, Taiwan, <sup>5</sup> Research Center for Emerging Viral Infections, Chang Gung University, Taoyuan, Taiwan

*Streptococcus pneumoniae* 19A ST320, a multidrug-resistant strain with high disease severity that notoriously spread before the use of expanded pneumococcal conjugate vaccines, was derived from a capsular switching event between an international strain Taiwan 19F-14 (ST236) and a serotype 19A strain. However, the molecular mechanisms underlying the adaptive evolution of 19F ST236 to 19A ST320 are unknown. In this study, we compared 19A ST320 to its ancestral clone, 19F ST236, in terms of adherence to respiratory epithelial cells, whole transcriptome, and ability to colonize a young mouse model. Serotype 19A ST320 showed five-fold higher adherence to A549 cells than serotype 19F ST236. High-throughput mRNA sequencing identified a prophage region located between *dnaN* and *ychF* in both strains; however, the genes in this region were expressed at significantly higher levels in 19A ST320 than in 19F ST236. Analysis by polymerase chain reaction (PCR) showed that the prophage is able to spontaneously excise from the chromosome and form a circular episome in 19A ST320, but not in 19F ST236. Deletion of the *integrase* in the prophage of 19A ST320 decreased spontaneous excision and cell adherence, which were restored by complementation. Competition experiments in mice showed that the *integrase* mutant was six-fold less competitive than the 19A ST320 parent (competitive index [CI]: 0.16;  $p = 0.02$ ). The 19A ST320 prophage-deleted strain did not change cell adherence capacity, whereas prophage integration strains (*integrase* mutant and 19F) had decreased expression of the down-stream *ychF* gene compared to that of 19A ST320. Further deletion of *ychF* significantly reduced cell adherence. In conclusions, these findings suggest that spontaneous prophage induction confers a competitive advantage to virulent pneumococci.

**Keywords:** *Streptococcus pneumoniae*, mRNA sequencing, phage, adherence, *integrase*

## INTRODUCTION

Prior to implementation of the 13-valent pneumococcal conjugate vaccine (PCV13 Prevnar 13, Pfizer), *Streptococcus pneumoniae* serotype 19A ST320 was prevalent in many countries (Choi et al., 2008; Moore et al., 2008; Ardanuy et al., 2009; Pillai et al., 2009; Shin et al., 2011; Hsieh et al., 2013). This clone emerged in South Korea before the introduction of seven-valent pneumococcal conjugate vaccine (PCV7) (Choi et al., 2008); surged in Taiwan, where only 20–30% of children < 5 years of age received  $\geq 1$  dose of PCV7 (Hsieh et al., 2013); and expanded as an important pathogen in the United States, Canada, and Spain after the widespread use of PCV7 (Moore et al., 2008; Ardanuy et al., 2009; Pillai et al., 2009). *S. pneumoniae* serotype 19A ST320 is resistant to multiple antibiotics, and is a frequent cause of invasive pneumococcal disease, pneumonia, acute otitis media, and haemolytic uremic syndrome (Copelovitch and Kaplan, 2010; Kaplan et al., 2010; Greenberg et al., 2011). It was suggested that the serotype 19A ST320 strain was derived from a capsular switching event that occurred between an international strain, Taiwan 19F-14 (ST236), and a serotype 19A strain (Moore et al., 2008). Although ST320 is a double-locus variant of ST236, serotype 19A ST320 is more virulent than its ancestral clone Taiwan 19F-14 (ST236) in terms of invasive potential and the severity of pneumonia (Hsieh et al., 2009, 2011). In our previous study, we demonstrated that the genetic evolution from Taiwan 19F-14 (ST236) to 19A ST320 has made this pneumococcus better able to colonize of the nasopharynx on a mouse model without vaccine and antibiotic use (Hsieh et al., 2013). This evolution reflects not only a switch in capsular serotype but also, more importantly, changes in other loci. The genetic change from ST236 to ST320 conferred a significant competitive advantage in nasopharyngeal colonization. Although the complete genome sequence of the serotype 19A ST320 clone has been determined<sup>1</sup>, the basis for its superior colonizing ability compared to that of Taiwan 19F-14 (ST236) is unclear. In this study, we used whole transcriptomic analysis via high-throughput mRNA-sequencing to study the mechanism responsible for the difference in colonization effectiveness between the 19A ST320 and 19F ST236 clones.

## MATERIALS AND METHODS

### Ethics Statement

Our animal procedures of this study were reviewed and approved by the Institutional Animal Care and Use Committee (IACUC) of Chang Gung University (Approval Number: CGU15-138), and the Committee recognizes that the proposed animal experiment follows the guideline as shown in the Guide for Laboratory Animal Facilities and Care as promulgated by the Council of Agriculture. Executive Yuan, ROC. BALB/cByJNarl mice were provided by National Laboratory Animal Center (NLAC), NARLabs, Taiwan. All animals were housed in an animal facility

at 22°C, with a relative humidity of 55%, in a 12 h light/12 h dark cycle, with sterile tap water and food available *ad libitum*.

### Strains and Growth Conditions

Pneumococcal isolates from Chang Gung Children's Hospital (CGCH) were grown at 37°C in Todd-Hewitt broth supplemented with 0.5% yeast extract (THY) or on blood agar supplemented with 5% defibrinated sheep blood in the presence of 5% CO<sub>2</sub>. *S. pneumoniae* is a biosafety level-2 microorganism. The experiments handling the bacteria should follow all appropriate guidelines and regulations. *Escherichia coli* was grown in Luria broth. Antibiotics were added at the following concentrations when required: spectinomycin at 250 mg/L for *S. pneumoniae* and 100 mg/L for *E. coli* and chloramphenicol at 4 mg/L for *S. pneumoniae* and 30 mg/L for *E. coli*.

### Cell Adhesion Assays

A549 (ATCC CCL-185) human lung epithelial carcinoma cells were grown in Dulbecco's modified Eagle's medium (DMEM; Gibco) supplemented with 10% fetal bovine serum (FBS, Gibco) at 37°C in a humidified incubator at 5% CO<sub>2</sub> and subcultured twice a week. Adhesion assays using A549 were performed as described previously (Nguyen et al., 2014), with some modification. Briefly, on the day before the adhesion assay, A549 cells were seeded in 24-well plates ( $1 \times 10^5$  cells/well) and maintained in culture medium at 37°C in a 5% CO<sub>2</sub> incubator. Mid-log phase (OD<sub>600</sub> = 0.4 to 0.6) *S. pneumoniae* in THY were washed once with serum-free DMEM medium and then added to each well at a multiplicity of infection (MOI) of 100 and co-incubated for 2 h at 37°C in a 5% CO<sub>2</sub> incubator. To determine the total numbers of adherent bacteria, the wells were washed three times with phosphate-buffered saline (PBS) to remove non-adhering bacteria, and 1 mL of deionized distilled water was added and incubated for 5 min to lyse cells. The adherent bacteria were enumerated by plating serial dilutions of the lysate on blood agar and counting the number of viable bacterial colony-forming units (CFUs). The experiments were performed in triplicate and repeated independently four times.

### Transcriptomic Analysis

For Illumina sequencing, total RNA was extracted from each sample (serotype 19A ST320 and Taiwan 19F-14 ST236) using the RNeasy mini kit (QIAGEN) and then treated with RNase-free DNase I (QIAGEN) for 15 min according to the manufacturer's protocols. The integrity of the isolated total RNA was checked using an Agilent Technologies 2100 Bioanalyzer. Then, cDNA libraries were prepared according to the manufacturer's instructions (Illumina), and an ABI StepOnePlus Real-Time PCR System was used for quantification and qualification of the sample library. The genome and gene information for serotype Taiwan 19F-14 ST236 and serotype 19A ST320 were downloaded from the NCBI database (accession numbers: CP000921.1 and CP001993.1, respectively). The expression level of each gene, as determined by RNA-Seq, was normalized to the number of reads per kilobase of exon region per million mapped reads (RPKM). The cut-off value for determining gene transcription

<sup>1</sup><http://www.ncbi.nlm.nih.gov/nuccore/CP001993.1>

was determined based on the 95% confidence interval for the RPKM values of each gene.

## Determination of mRNA Expression Levels by Quantitative Reverse Transcription Polymerase Chain Reaction (RT-qPCR)

An aliquot (400 ng) of total RNA from each bacterial strain was subjected to cDNA synthesis using SuperScript IV Reverse Transcriptase (Thermo Fisher). The cDNAs of *HMPREF0837\_10263*, *HMPREF0837\_10266*, *dnaN*, *ychF* and 23S rRNA were quantified using KAPA SYBR® FAST qPCR Master Mix (KAPA Biosystems) and an ABI 7900 Real-Time PCR system. The cycling conditions for the quantitative real-time PCR (qPCR) were as follows: 50°C for 2 min and 95°C for 2 min, followed by 50 cycles of 95°C for 15 s and 60°C for 30 s, and after 50 cycles, melting curve analysis was performed from 60°C to 95°C, with a 2% ramp rate. Sequences of the primers used for RT-qPCR are listed in Table 1. The relative mRNA expression levels were calculated according to the  $\Delta\Delta C_t$  method, with normalization to 23S rRNA levels.

## Determining the Population With Excised Prophage by Quantitative Real-Time PCR (qPCR)

The population with excised prophage were determined by qPCR. The following oligonucleotide pairs were designed for the experiment: prophage-excised-specific oligonucleotides to amplify a 151-bp fragment (RT-A/RT-B) near the *attB* site on the chromosome; non-prophage-specific oligonucleotides designed to amplify a 72-bp fragment (RT-10621-F/RT-10621-R) of *HMPREF0837\_10621*. First, 19A ST320 genomic DNA was used as a template to amplify target gene fragments by PCR using the primer pairs 10621-F/10621-R (724-bp, SP\_10621, for the non-prophage genomic region) and A/B (2,290-bp, EC, for the excised chromosomal DNA, “*attB*”), which were then cloned into pJET1.2/blunt (Thermo Fisher) to create plasmid standards for each target (named 10621/pJET and EC/pJET, respectively). Each amplification was carried out in a 20  $\mu$ l reaction containing KAPA SYBR® FAST qPCR Master Mix on an ABI 7900 system. Serial 10-fold dilutions of the plasmid standard containing  $0.1-1 \times 10^6$  copies were used to establish a standard curve to evaluate the Ct V.S.  $\log_{10}$ (copy number). To determine the changes in prophage excision over time, a culture of 19A ST320 was grown in THY at 37°C and 5% CO<sub>2</sub> and genomic DNA was extracted at different time points. Then, the percentage of cells with excised prophage at each time point were analyzed by qPCR and normalized to the standard curve. To estimate the cell population with excised prophage at different time points, the number of copies of excised-chromosomal target region was divided by the number of copies of SP\_10621 at each time point.

## Construction of Deletion Mutants

The *integrase* (*int*), *dnaN* and *ychF* gene-deletion strain (19A- $\Delta int$ , 19A- $\Delta dnaN$  and 19A- $\Delta ychF$ ) was generated by replacing the gene with a spectinomycin resistance gene cassette as follow

**TABLE 1** | Primers and plasmids used in this work.

Primer name	Sequence (5' to 3')	Purpose
int-up-F	ATG GAA CTC CAA CAG TAC GAT G	$\Delta int$
int-dn-R	ATA TGA CAT GGT TAC TGC ACG A	
int-inverse-F	GGT TTT ACT CCT TTT TCC ATC	$\Delta int$ (iPCR)
int-inverse-R	TAA AAA AGT CCA TAA AAT TAT TAT TTC	
ychF-up-F	CAA AAC CTT TTC TAA TTG CTT G	$\Delta ychF$
ychF-dn-R	ACA ATA CTA TCT TTG AAT GC	
ychF-inverse-F	TCT CCG TTT TCA TTT CAA TCC	$\Delta ychF$ (iPCR)
ychF-inverse-R	AAA TTA ATA AAT GGT GTC AAT TAG G	
dnaN-up-F	GTA AGA CTC ACT TAT TAA ACG	$\Delta dnaN$
dnaN-dn-R	TTG CAA CTT TAG AAA GTG G	
dnaN-inverse-F	GGA TTC TCC TTT ATT TAT TTT TAG	$\Delta dnaN$ (iPCR)
dnaN-inverse-R	GTG AAA GAG GTT GAG CCT G	
Spec-F	GTG AGG AGG ATA TAT TTG AAT AC	Spectinomycin
Spec-R	TTA TAA TTT TTT TAA TCT GTT ATT TAA ATA GTT TAT AG	
Pint-F	AGA AAA TGA AGA AAA TTG TTT	$\Delta int:int$
int-R	TTT TTC ATA AAA TGA AGT AGC	
Pcat-F	GTG ATA TAG ATT GAA AAG	Chloramphenicol
cat-R	TTA TTT ATT CAG CAA GTC	
12133-F	TTG CAA GAT AAG ATT ATC CAG	$\Delta int:int$
12136-R	TTA AAC GGA TAT TCT TTA GAG	
12134-5-inverse-F	TAT TAA ACG ATA TAA GTT TG	$\Delta int:int$ (iPCR)
12134-5-inverse-R	CAA AAA ATA CGA AAA TGA TTA G	
10621-F	GAT TGA GAT CCA TTG AAACG	SP_10621
10621-R	AGA GAA CGT GTA ATC CCT GAA C	
C	ATG GAA CTC CAA CAG TAC GAT G	EP region
D	TCT TAT AAG TGT TCT GAA GC	
A	TGA AGA TGC TGG TTT GTT A	EC region
B	ATA TGA CAT GTT ACT GCA CGA	
RT-10621-F	CCC AGG GCT TGC AAA TTA CA	qPCR
RT-10621-R	CGA TCA TGT TGC CAG TTC GA	
RT-A	GCG ATA TGA TTT TGA GCG AAA A	qPCR
RT-B	CAA CGA TAC CTG CTG TCA AAG C	
RT-10263-F	CGT TCT TCA AAT GCT TCA TCG T	RT-qPCR
RT-10263-R	CGT ATC CGT GAC GGT TTC AA	
RT-10266-F	CCC CGT TTT CGC CTT GT	RT-qPCR
RT-10266-R	CCC CGT TTT CGC CTT GT	
RT-ychF-F	CGC GTG CAG CTT ACC ACTT	RT-qPCR
RT-ychF-R	CAA GCG CGA ACT TCT TTT TCA	
RT-dnaN-F	TCA GCT GTT CGT CCA TTT ACT CTT	RT-qPCR
RT-dnaN-R	TTA ATT TGT ACG AAC TGG TG	
RT-23S-F	ATG CGA CGA GCC GAC ATC	RT-qPCR
RT-23S-R	CCC CCA AGA GTT CAC ATC GA	
Plasmid	Features	Reference
pDL278	<i>spec<sup>R</sup></i> ; <i>E. Coli</i> -Streptococcus shuttle vector	(LeBlanc et al., 1992)
pKO3-Km	<i>cat<sup>R</sup></i> and <i>km<sup>R</sup></i> ; pKO3-derived plasmid	(Pan et al., 2008)
pGEM-T easy	T-A cloning vector	Promega
pJET1.2/blunt	Cloning vector	Thermo Fisher

and primer used are listed in Table 1. Briefly, coding regions and flanking fragments for *int*, *dnaN* and *ychF* form the serotype 19A ST320 were amplified by PCR using primer pairs:

int-up-F/int-dn-R for *int*, dnaN-up-F/dnaN-dn-R for *dnaN* and ychF-up-F/ychF-dn-R for *ychF*, respectively. The resulting PCR products were cloned into a pGEM<sup>®</sup>-T easy (Promega) plasmid. The coding regions of the *int*, *dnaN* and *ychF* were then removed by inverse PCR (iPCR) with primer pairs: int-inverse-F/int-inverse-R for  $\Delta int$ , dnaN-inverse-F/dnaN-inverse-R for  $\Delta dnaN$  and ychF-inverse-F/ychF-inverse-R for  $\Delta ychF$ , respectively and ligated to a PCR amplified spectinomycin antibiotic cassette (spec-F/spec-R) from pDL278 plasmid to create a deletion construct vector. This vector was transformed into *S. pneumoniae* serotype 19A ST320 by Competence Stimulating Peptide-1 (CSP-1; GenScript), and transformants were selected on spectinomycin.

## Construction of an *integrase* Complementation Strain

To construct a complemented 19A ST320 *integrase* deletion mutant strain (19A- $\Delta int::int$ ), a single copy of the *integrase* gene was inserted into the non-coding region between the HMPREF0837\_12134 and HMPREF0837\_12135 as follows. The *integrase* gene was PCR amplified from 19A ST320 by using the primer pair Pint-F/int-R, and then cloned into the pGEM<sup>®</sup>-T easy plasmid to generate Pint::pGEM-T. A chloramphenicol (*cat*) antibiotic cassette from pKO3-Km plasmid was PCR amplified by using the primer pair Pcat-F/cat-R, and then sub-cloned into the SacII site of Pint::pGEM-T to generate Pint-*cat*::pGEM-T. Then, the primer pair Pint-F/cat-R was used to produce a Pint-*cat* PCR fragment. Next, a 2,501-bp fragment of the insertion site was PCR amplified by using the primer pair 12133-F/12136-R and cloned into pGEM<sup>®</sup>-T easy to create p12133-12136::pGEM-T. A fragment generated by iPCR using the above plasmid and the primer pair 12134-5-inverse-F/12134-5-inverse-R was then ligated with the Pint-*cat* PCR fragment to form the complementation vector p12133-Pint-*cat*-12136::pGEM-T. The complementation strain ( $\Delta int::int$ ) was created by transforming the p12133-Pint-*cat*-12136::pGEM-T plasmid into the 19A- $\Delta int$  strain using CSP-1 and selecting on chloramphenicol.

## In vivo Competition Assays

An *in vivo* competition assay for *S. pneumoniae* infection in mice was conducted as described previously (Hsieh et al., 2013). Mid-log phase (OD<sub>600</sub> = 0.2–0.6) bacteria were combined at a 1:1 ratio (CFUs) in PBS, and the inoculating doses were confirmed by plating on blood agar plates. Then, 3-week-old female BALB/c mice were challenged intranasally (IN) with 50  $\mu$ L of bacteria (containing  $5 \times 10^6$  CFUs/bacterial strain). After 7 days, the mice were sacrificed with CO<sub>2</sub>, and nasal lavages fluid was collected. The CFUs recovered were determined by serial dilution and plating on blood agar. For the competition experiment between wild-type strain and the *integrase* deletion mutant, the recovered bacteria were distinguished by replica plating on blood agar containing 250 mg/L spectinomycin. One hundred randomly picked colonies were tested per mouse. A competitive index (CI) was calculated based on the ratio of the competing bacterial strains recovered by nasal lavage, normalized to the ratio of the respective

bacteria in the inoculum = (output<sub>test strain</sub>/output<sub>wild type</sub>)/(input<sub>test strain</sub>/input<sub>wild type</sub>).

## Statistical Analysis

Data are presented as means  $\pm$  standard deviation (SD) from more than three independent experiments. Statistical significance was assessed by a two-tailed Student's *t*-test. The mouse CI assay was analyzed by a one-sample Student's *t*-test (one-tailed) using log-transformed CIs to determine if the indices were significant. A *p* value less than 0.05 was considered statistically significant. All statistical analyses were performed using SPSS 15.0 for Windows (Statistical Package for Social Sciences, Chicago, IL, United States).

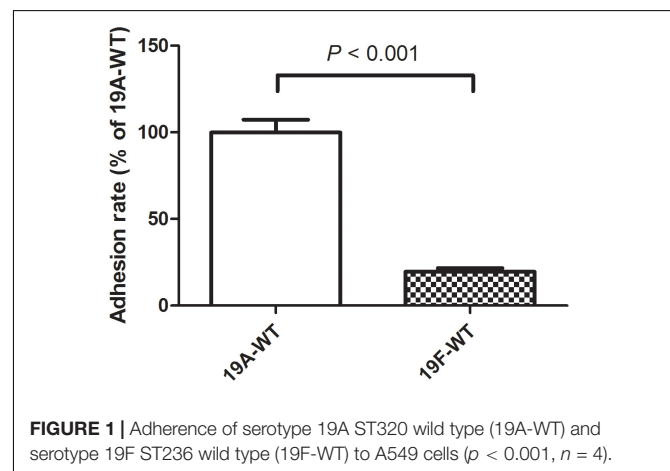
## RESULTS

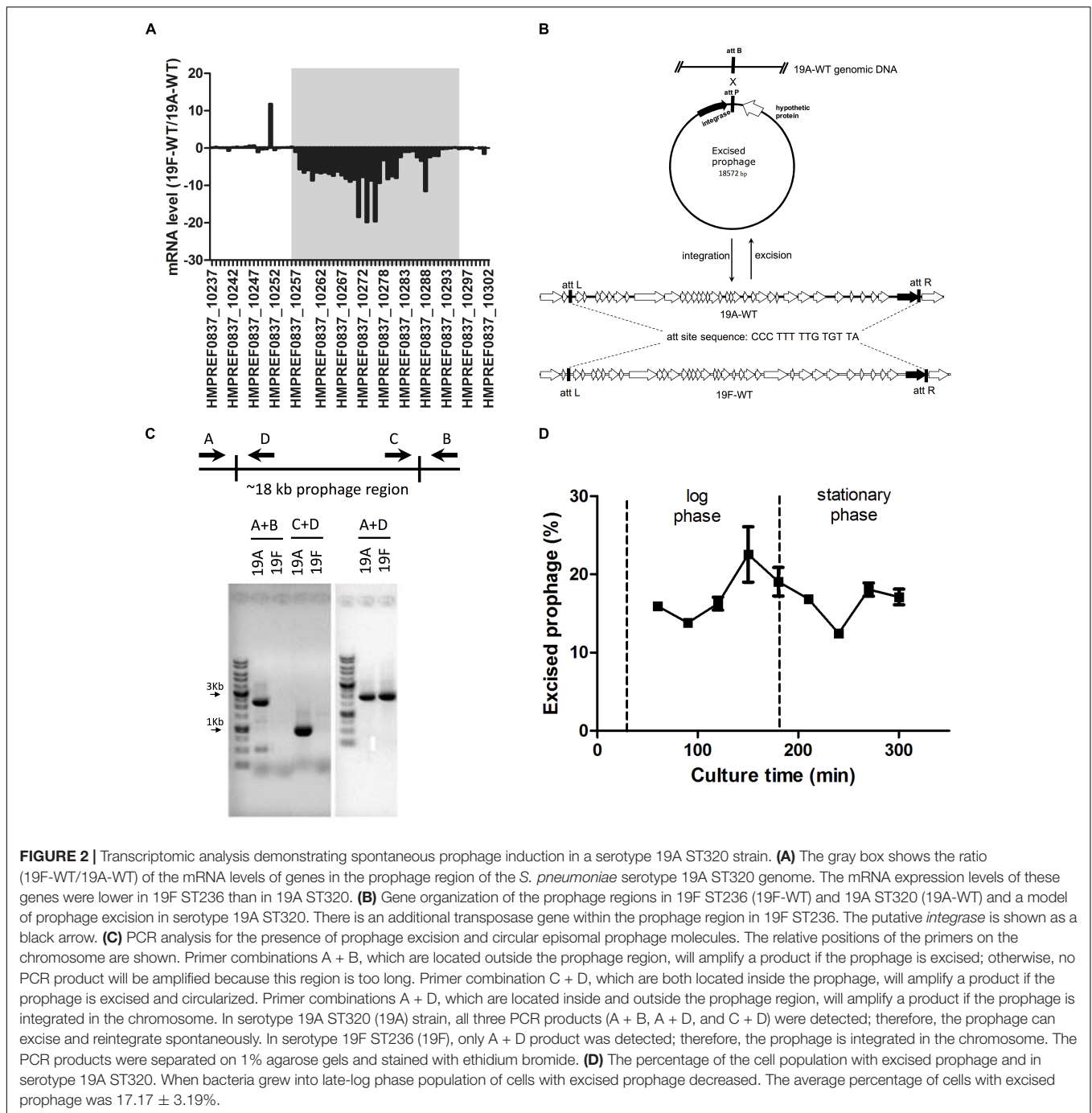
### More Serotype 19A ST320 Cells Adhered to A549 Cells Than Serotype 19F ST236 Cells

In a previous study, we demonstrated that the serotype 19A ST320 strain exhibited higher colonizing ability than its ancestral clone Taiwan 19F-14 (ST236) in mice (Hsieh et al., 2013). In this study, we demonstrated that the serotype 19A ST320 strain showed five-fold higher adherence to A549 cells than the serotype 19F ST236 strain (*p* < 0.001) (Figure 1).

### Transcriptomic Analysis

The transcriptomic analysis revealed 801 genes that were differentially expressed between the serotype 19A ST320 and 19F ST236 strains, including 641 and 160 genes that were upregulated and downregulated in serotype 19A ST320, respectively (Supplementary Table S1 and Supplementary Figure S1). Of note, the mRNA levels of many genes located in the prophage region (~18 kb) between HMPREF0837\_10256 (*dnaN*, encoding DNA polymerase III beta subunit) and HMPREF0837\_10294 (*ychF*, encoding a GTP-binding protein) were significantly higher in 19A ST320 than in 19F ST236 (Figure 2A). A RT-qPCR assay was then conducted on two





genes within the prophage region (*HMPREF0837\_10263* and *HMPREF0837\_10266*) to verify the RNA-seq results. RT-qPCR confirmed an increase in the mRNA levels of these two genes in 19A ST320 compared to the corresponding levels in 19F ST236 (data not shown).

There are 34 open reading frames (ORFs) located within the prophage region in 19A ST320 and 19F ST236 (Figure 2B). But, there was an additional transposase gene in the prophage region in 19F ST236. A 14-bp direct repeat sequence “5'-CCC TTT TTG TGT TA-3'” flanked the prophage region, which should

be the insertion site of this prophage. The GC content of the approximately 18 kb prophage region is 38%. These two strains shared 99% nucleotide identity in this prophage region.

### Demonstration of Epichromosomal Circular Prophage DNA in Serotype 19A ST320

We hypothesized that there was increased spontaneous prophage induction in 19A ST320, which accounted for the difference

in mRNA levels of genes within the prophage between 19A ST320 and 19F ST236. PCR with several combinations of primers was used to assess spontaneous integration and excision of the prophage region in 19A ST320. If the prophage could excise from the bacterial chromosome to form an epichromosomal circular structure, the PCR products would be observed using primer pairs A/B (2,290-bp) and C/D (901-bp) (Figure 2C). PCR with the primer pair A/D (1,914-bp) would yield a product when the prophage is integrated into the bacterial chromosome (Figure 2C). In our experiment, we found that the prophage excise from the genome and exist as a double-stranded circular DNA molecule in the serotype 19A ST320 strain by PCR; whereas the prophage was integrated in the genome of the serotype 19F ST236 strain (Figure 2C). A DNA sequence analysis of the PCR fragments produced by primer pairs A/B and C/D confirmed the ends of the circular phage DNA were connected via one of the 14-bp direct repeat sequence (5'-CCC TTT TTT TGT TA-3') flanking the prophage region (C/D); the other one 14-bp direct repeat was left in the chromosome (A/B) when the prophage region excised from the serotype 19A ST320 genome. We also tested for excision activity in 10 other serotype 19A ST320 isolates and 8 serotype 19F ST236 isolates by PCR. The results showed that all serotype 19A ST320 isolates had spontaneous prophage induction. Two of the eight serotype 19F ST236 isolates did not harbor the prophage, whereas the other six isolates had the prophage, but no spontaneous induction was observed (Table 2). Another 19 clinical isolates belonging to different serotypes were also examined. The results showed that these 19 clinical isolates did not contain the prophage (Table 2).

## The Percentage of Cells in a Population With Excised Prophage

Bacterial cells were harvested at different growth phases, from early log phase to stationary phase, we found that the percentage of the cell population with excised prophage increased with cell

growth into late-log phase, but decreased at stationary phase. The average percentage of cells with excised prophage across all culture time points was  $17.17 \pm 3.19\%$  (Figure 2D).

## Spontaneous Prophage Induction Depends on *integrase* and Is Associated With Increased Adherence to Respiratory Epithelial Cells

The prophage region of 19A ST320 harbors a putative *integrase* gene at the 3' end (Figure 2B). The *integrase* gene was deleted to study whether it was responsible for prophage excision and integration. Following deletion of the *integrase* gene in 19A ST320, no prophage excision was detectable by PCR in 19A ST320 isogenic *integrase* mutant (19A- $\Delta$ *int*) (Figure 3A). Complementation of the deletion with an *integrase* gene at another chromosomal location (19A- $\Delta$ *int*::*int*) restored prophage excision (Figure 3A). Also, the mRNA expression level of genes (*HMPREF0837\_10263* and *HMPREF0837\_10266*) within the prophage region in the *integrase* deletion mutant (19A- $\Delta$ *int*) were significantly lower than that in 19A ST320 wild type ( $p < 0.05$ ) (Figure 3B).

The growth curves and CFUs in different phases of the *integrase* deletion mutant and 19A ST320 wild type were similar (Figure 4A). We tested whether prophage excision is associated with adherence because there was a difference in adherence to respiratory epithelial cells between the serotype 19A ST320 and 19F ST236 strains (Figure 1). The isogenic *integrase* deletion mutant (19A- $\Delta$ *int*) of serotype 19A ST320 showed decreased adherence to A549 cells compared to the wild-type strain ( $p < 0.002$ ), whereas the *integrase* complementation strain (19A- $\Delta$ *int*::*int*) showed restored cell adherence capacity that was similar to the wild-type strain ( $p = 0.8$ ) (Figure 4B).

## Nasopharyngeal Colonization Competition in Young Mice

To reduce the variance caused by differences among mice, we performed a competition experiment in which mice were inoculated intra-nasal (IN) with equal CFUs of serotype 19A ST320 (19A-WT) and the isogenic *integrase* deletion mutant (19A- $\Delta$ *int*) to assess the role of prophage excision on colonization. At 7 days post-infection, the isogenic *integrase* deletion mutant (19A- $\Delta$ *int*) was sixfold less competitive than the parent serotype 19A ST320 strain in colonizing the mouse upper airway (CI = 0.16;  $p = 0.02$ ; Figure 4C).

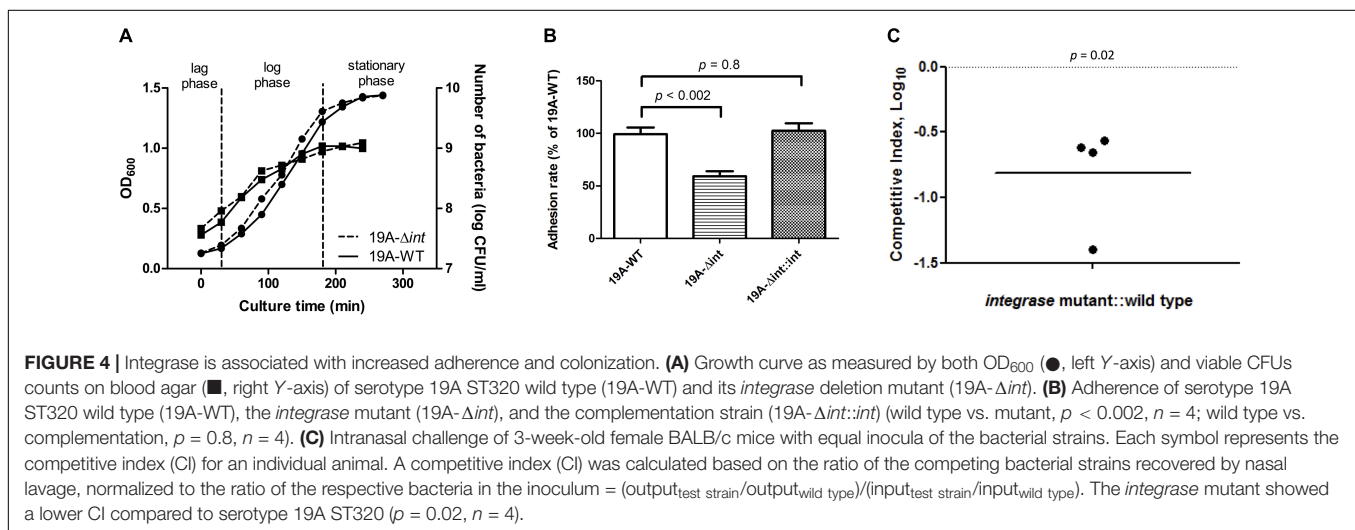
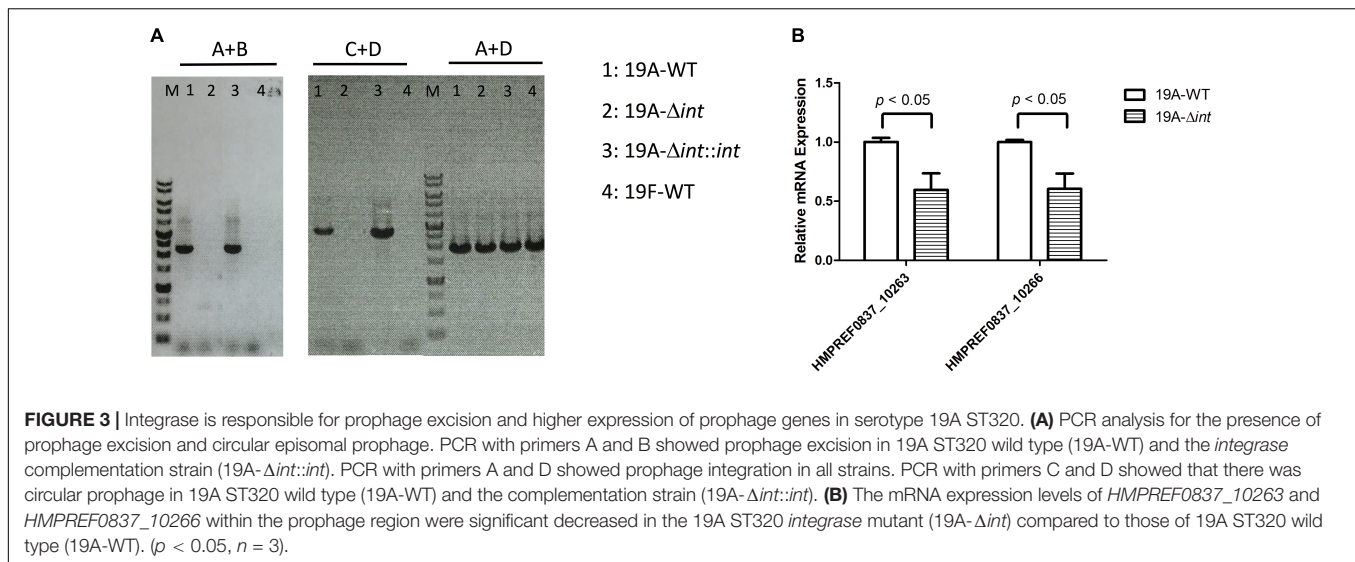
## Prophage Integration Decreased the Expression of the Downstream *ychF* Gene Which Was Associated With Cell Adherence

We created a 19A ST320 mutant devoid of the prophage region (19A- $\Delta$ phage) to test whether the circular prophage DNA molecule directly modulates bacterial adherence. No difference was found in adhesion ability between the serotype 19A ST320 (19A-WT) and the prophage deletion mutant (19A- $\Delta$ phage) ( $p = 0.9$ ) (Figure 5A). This result indicated that the circular

**TABLE 2** | The presence of prophage and prophage excision in clinical isolates of serotype 19A ST320, 19F ST236, and others serotypes.

Serotype	Numbers of isolates (n)	PCR products			Interpretation
		A + B	C + D	A + D	
19A	10	+	+	+	Prophage excision, integration
19F	6	-	-	+	Prophage integration, no excision
19F	2	+	-	-	No prophage
6B	3	+	-	-	No prophage
15A	2	+	-	-	No prophage
14	4	+	-	-	No prophage
23F	3	+	-	-	No prophage
15B	1	+	-	-	No prophage
3	6	+	-	-	No prophage

+, PCR positive; -, PCR negative.



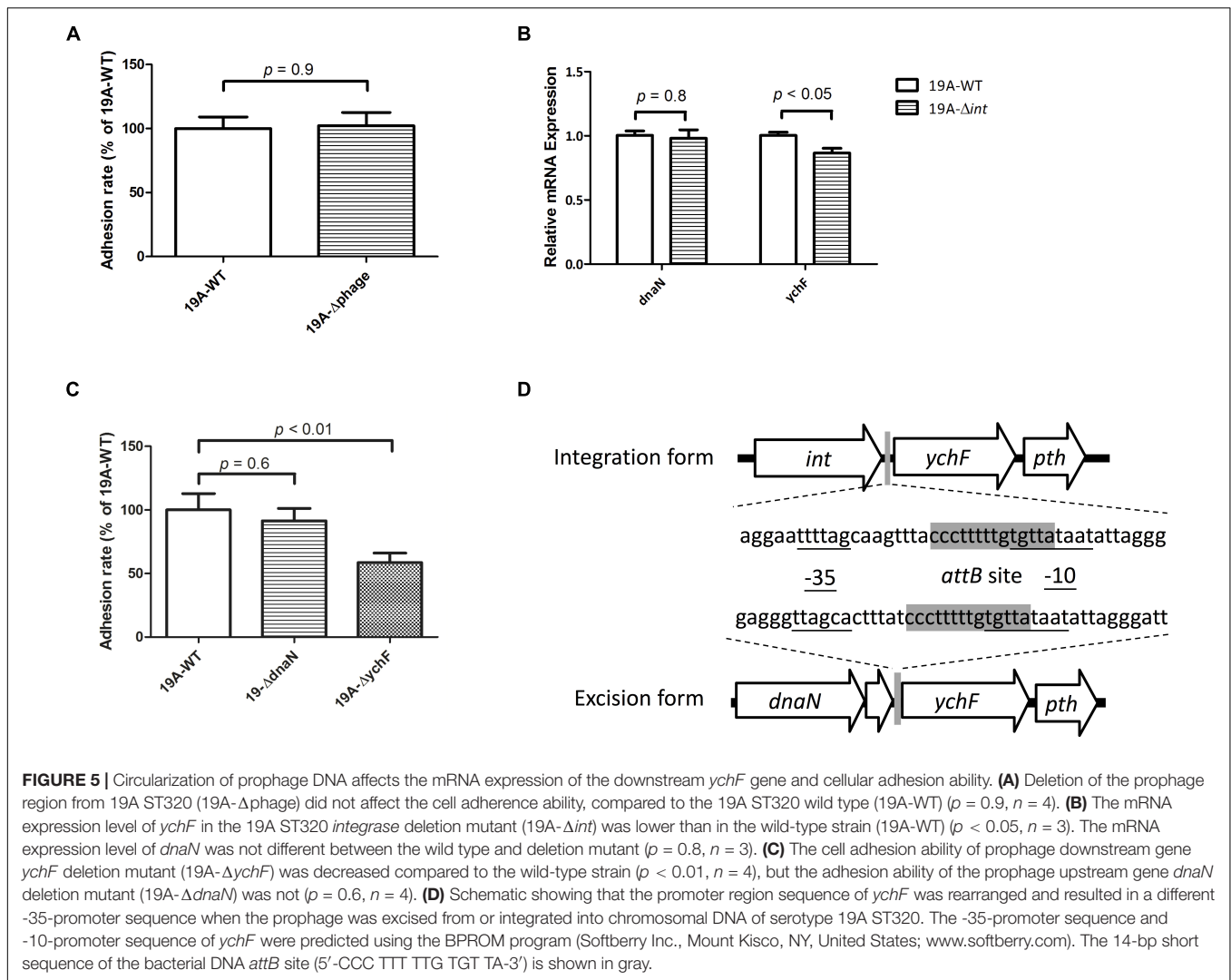
prophage, on its own, did not directly impact cell adherence. Next, we found that the mRNA expression level of *ychF* was different between strains 19A-WT and 19A- $\Delta$ *int* ( $p < 0.05$ ) (Figure 5B). Transcriptome analysis also showed that the mRNA level of *ychF* was higher in serotype 19A ST320 than in 19F ST236. To analyze the bacterial adherence ability, as compared to the wild-type strain, we generated a 19A ST320 *ychF* deletion mutant (19A- $\Delta$ *ychF*). Deletion of *ychF* in the 19A ST320 strain did not impact growth (data not shown). However, 19A- $\Delta$ *ychF* had a lower bacterial adherence ability than 19A-WT ( $p < 0.01$ ) (Figure 5C). The -35-promoter sequence of *ychF* is rearranged when the prophage region integrates into or excises from chromosomal DNA of serotype 19A ST320 (Figure 5D).

## DISCUSSION

ST320 is the most predominant clone among 19A serotype *S. pneumoniae* isolates in both eastern and western countries

(Beall et al., 2011; Shin et al., 2011). The high antibiotic resistance rates among ST320 strains are assumed to be one of the major reasons for its widespread dissemination and expansion. In response to antibiotic stress, *S. pneumoniae* shows a high rate of genetic transformation, which promotes the evolution of virulence (Prudhomme et al., 2006). In order to understand how the serotype 19A ST320 clone became an effective colonizer, we compared the serotype 19F ST236 clone to the serotype 19A ST320 clone and found that the mechanism of spontaneous prophage induction contributed to the competitive advantage of the serotype 19A ST320 clone. Through prophage excision and integration, the dynamic process act as a molecular switch that regulates the expression of *ychF* to increase bacterial adherence and drove the emergence of serotype 19A ST320 clone.

Bacteriophage, the most abundant biological entity on earth, play a crucial role in bacterial survival, activity and evolution (Rohwer and Edwards, 2002). Many bacterial genomes contain phage DNA, which may encode a virulence factor or increase



bacterial fitness (Waldor, 1998). In fact, prophage acquisition has shaped the epidemiology of important bacterial pathogens (Banks et al., 2002). Residing in the ecological niche, the prophage is integrated into the bacterial chromosome of the serotype 19F ST236 clone, which decreased the expression of the downstream *ychF* gene. In serotype 19A ST320 clone, this prophage evolved to spontaneously excise from the chromosome, and this excision event was associated with increased expression of the downstream *ychF* gene, cell adherence and colonizing ability. Two direct 14-bp repeats flanking the prophage region (5'-CCC TTT TTG TGT TA-3') were identified as the specific site of prophage integration. The gene encoding *integrase*, located at the 3' junction of the prophage in serotype 19A ST320 strains, catalyzes the site-specific recombination between the prophage recognition site (*attP*) and a short sequence of bacterial DNA (*attB*) in serotype 19A ST320 strains. Several phages integrate their genome into the bacterial chromosome and exist in a lysogenic state, or replicate and lyse the bacterial host after induction. There are two lysogenic processes in which bacteria and phage interact: lysogenic conversion and

active lysogeny. When the expression of phage-encoded proteins changes the bacterial phenotype and/or contributes to bacterial fitness, this is called lysogenic conversion, which is observed in *Corynebacterium diphtheria*, with the expression of diphtheria toxin; in *E. coli* O157:H7, with the expression of shiga toxins; and in *Vibrio cholera*, with the expression of cholera toxin (Freeman, 1951; Waldor and Mekalanos, 1996; Plunkett et al., 1999). In active lysogeny, an integrated prophage serves as a regulatory switch that controls the expression of bacterial genes, which is observed with the *comK* gene in *Listeria monocytogenes* and the mismatch repair system (MMR) in *Streptococcus pyogenes* (Rabinovich et al., 2012; Scott et al., 2012). Serotype 19F ST236 strains carry the prophage region, like serotype 19A ST320. Deletion of the prophage in serotype 19A ST320 did not change the cell adherence ability. The cooperative behavior between 19A ST320 and the prophage is likely to be active lysogeny. The prophage, upon integration into the genome of serotype 19A ST320, alters the expression of the *ychF* gene, probably via genome rearrangement of the promoter sequences. YchF, a conserved GTPase, has been shown to impact pneumococcal

growth and virulence (Fernebro et al., 2008). In this study, we also found that YchF was involved in adherence to respiratory epithelial cells.

Despite numerous attempts, we could not isolate any phage particles from the culture medium of serotype 19A ST320 strains following UV irradiation and mitomycin C induction (data not shown). As we did not observe any phage structural genes, genes for DNA packaging, or the holing/lysin system for bacterial lysis, the prophage in the 19A ST320 strain did not seem to enter the lytic cycle and release new virions. However, the prophage has the replication protein and primase necessary for DNA replication. Increased mRNA expression of the prophage region in serotype 19A ST320 compared to serotype 19F ST236 is likely due to replication of the circular prophage genome as an autonomous element, just like the prophage CGP3 in *Corynebacterium glutamicum* and SF370.4 in *Streptococcus pyogenes* (Frunzke et al., 2008; Scott et al., 2008). The purpose of phage replication is to prevent its elimination from the bacterial population. In this study, we characterized the excisional activity of the 18kb prophage and evaluated its impact on pneumococcal adherence during colonization. However, the upstream events that lead to the activation of prophage excision and other phage-mediated mechanism relevant to colonization in serotype 19A ST320 strains remain unclear. Further studies are required to elucidate the mutually beneficial relationship between the bacteria and phages.

The availability and use of pneumococcal conjugate vaccines has dramatically decreased the incidence of invasive diseases caused by vaccine-targeted serotypes (Harboe et al., 2014). Nevertheless, the conjugate vaccines target only a small subset (up to 13) of the >90 known capsular serotypes of *S. pneumoniae*. This decline in the incidence of pneumococcal diseases caused by vaccine serotypes has been offset by substantial increases in both the carriage of and diseases caused by non-vaccine serotypes, which now occupy the niche vacated by vaccine-type pneumococci (Hicks et al., 2007; Singleton et al., 2007). Thus,

vaccine-induced serotype replacement is gradually occurring (Chochua et al., 2017; Ladhani et al., 2018; Nakano et al., 2018). Moreover, certain successful lineages that were prevalent before the use of PCV, such as ST156, can persist after PCV implementation by undergoing capsular switching with a non-vaccine serotype (35B) (Chochua et al., 2017). The genome plasticity of pneumococci is high; therefore, it is an evolving threat to human health worldwide. Understanding the phage-related mechanisms that confer pneumococcal adaptation and pathogenicity offers a valuable perspective in our fight against pneumococcal disease.

## AUTHOR CONTRIBUTIONS

Y-YC, J-TW, T-LL, and Y-CH designed the research, discussed the analysis, and revised the paper. Y-YC, T-HL, and Y-YH prepared materials and performed the experiments. Y-YC, T-LL, and Y-NG analyzed the data. Y-YC and Y-CH wrote the main text of the manuscript. All the authors reviewed and approved the final version of the manuscript.

## FUNDING

This study was supported in part by grants from the Ministry of Science and Technology (105-2314-B-182-049-MY3) and the Chang Gung Memorial Hospital (CMRPG3G1221 and CMRPG3F1871-1872) in Taiwan.

## SUPPLEMENTARY MATERIAL

The Supplementary Material for this article can be found online at: <https://www.frontiersin.org/articles/10.3389/fmicb.2019.00205/full#supplementary-material>

## REFERENCES

- Ardanuy, C., Rolo, D., Fenoll, A., Tarrago, D., Calatayud, L., and Linares, J. (2009). Emergence of a multidrug-resistant clone (ST320) among invasive serotype 19A pneumococci in Spain. *J. Antimicrob. Chemother.* 64, 507–510. doi: 10.1093/jac/dkp210
- Banks, D. J., Beres, S. B., and Musser, J. M. (2002). The fundamental contribution of phages to GAS evolution, genome diversification and strain emergence. *Trends Microbiol.* 10, 515–521. doi: 10.1016/S0966-842X(02)02461-7
- Beall, B. W., Gertz, R. E., Hulkower, R. L., Whitney, C. G., Moore, M. R., and Brueggemann, A. B. (2011). Shifting genetic structure of invasive serotype 19A pneumococci in the United States. *J. Infect. Dis.* 203, 1360–1368. doi: 10.1093/infdis/jir052
- Chochua, S., Metcalf, B. J., Li, Z., Walker, H., Tran, T., McGee, L., et al. (2017). Invasive serotype 35B pneumococci including an expanding serotype switch lineage, United States, 2015–2016. *Emerg. Infect. Dis.* 23, 922–930. doi: 10.3201/eid2306.170071
- Choi, E. H., Kim, S. H., Eun, B. W., Kim, S. J., Kim, N. H., Lee, J., et al. (2008). *Streptococcus pneumoniae* serotype 19A in children, South Korea. *Emerg. Infect. Dis.* 14, 275–281. doi: 10.3201/eid1402.070807
- Copelovitch, L., and Kaplan, B. S. (2010). *Streptococcus pneumoniae*-associated hemolytic uremic syndrome: classification and the emergence of serotype 19A. *Pediatrics* 125, e174–e182. doi: 10.1542/peds.2007-2017
- Fernebro, J., Blomberg, C., Morfeldt, E., Wolf-Watz, H., Normark, S., and Normark, B. H. (2008). The influence of *in vitro* fitness defects on pneumococcal ability to colonize and to cause invasive disease. *BMC Microbiol.* 8:65. doi: 10.1186/1471-2180-8-65
- Freeman, V. J. (1951). Studies on the virulence of bacteriophage-infected strains of *Corynebacterium diphtheriae*. *J. Bacteriol.* 61, 675–688.
- Frunzke, J., Bramkamp, M., Schweitzer, J. E., and Bott, M. (2008). Population heterogeneity in *Corynebacterium glutamicum* ATCC 13032 caused by prophage CGP3. *J. Bacteriol.* 190, 5111–5119. doi: 10.1128/JB.00310-08
- Greenberg, D., Givon-Lavi, N., Newman, N., Bar-Ziv, J., and Dagan, R. (2011). Nasopharyngeal carriage of individual *Streptococcus pneumoniae* serotypes during pediatric pneumonia as a means to estimate serotype disease potential. *Pediatr. Infect. Dis. J.* 30, 227–233. doi: 10.1097/INF.0b013e3181f87802
- Harboe, Z. B., Dalby, T., Weinberger, D. M., Benfield, T., Molbak, K., Slotved, H. C., et al. (2014). Impact of 13-valent pneumococcal conjugate vaccination in invasive pneumococcal disease incidence and mortality. *Clin. Infect. Dis.* 59, 1066–1073. doi: 10.1093/cid/ciu524
- Hicks, L. A., Harrison, L. H., Flannery, B., Hadler, J. L., Schaffner, W., Craig, A. S., et al. (2007). Incidence of pneumococcal disease due to non-pneumococcal conjugate vaccine (PCV7) serotypes in the United States during the era of

- widespread PCV7 vaccination, 1998–2004. *J. Infect. Dis.* 196, 1346–1354. doi: 10.1086/521626
- Hsieh, Y. C., Lin, P. Y., Chiu, C. H., Huang, Y. C., Chang, K. Y., Liao, C. H., et al. (2009). National survey of invasive pneumococcal diseases in Taiwan under partial PCV7 vaccination in 2007: emergence of serotype 19A with high invasive potential. *Vaccine* 27, 5513–5518. doi: 10.1016/j.vaccine.2009.06.091
- Hsieh, Y. C., Lin, T. L., Chang, K. Y., Huang, Y. C., Chen, C. J., Lin, T. Y., et al. (2013). Expansion and evolution of *Streptococcus pneumoniae* serotype 19A ST320 clone as compared to its ancestral clone, Taiwan 19F-14 (ST236). *J. Infect. Dis.* 208, 203–210. doi: 10.1093/infdis/jit145
- Hsieh, Y. C., Wang, C. W., Lai, S. H., Lai, J. Y., Wong, K. S., Huang, Y. C., et al. (2011). Necrotizing pneumococcal pneumonia with bronchopleural fistula among children in Taiwan. *Pediatr. Infect. Dis. J.* 30, 740–744. doi: 10.1097/INF.0b013e31821b10c3
- Kaplan, S. L., Barson, W. J., Lin, P. L., Stovall, S. H., Bradley, J. S., Tan, T. Q., et al. (2010). Serotype 19A is the most common serotype causing invasive pneumococcal infections in children. *Pediatrics* 125, 429–436. doi: 10.1542/peds.2008-1702
- Ladhani, S. N., Collins, S., Djennad, A., Sheppard, C. L., Borrow, R., Fry, N. K., et al. (2018). Rapid increase in non-vaccine serotypes causing invasive pneumococcal disease in England and Wales, 2000–17: a prospective national observational cohort study. *Lancet Infect. Dis.* 18, 441–451. doi: 10.1016/S1473-3099(18)30052-5
- LeBlanc, D. J., Lee, L. N., and Abu-Al-Jaibat, A. (1992). Molecular, genetic, and functional analysis of the basic replicon of pVA380-1, a plasmid of oral streptococcal origin. *Plasmid* 28, 130–145. doi: 10.1016/0147-619X(92)90044-B
- Moore, M. R., Gertz, R. E. Jr., Woodbury, R. L., Barkocy-Gallagher, G. A., Schaffner, W., Lexau, C., et al. (2008). Population snapshot of emergent *Streptococcus pneumoniae* serotype 19A in the United States, 2005. *J. Infect. Dis.* 197, 1016–1027. doi: 10.1086/528996
- Nakano, S., Fujisawa, T., Ito, Y., Chang, B., Matsumura, Y., Yamamoto, M., et al. (2018). Spread of meropenem-resistant *Streptococcus pneumoniae* serotype 15A-ST63 clone in Japan, 2012–2014. *Emerg. Infect. Dis.* 24, 275–283. doi: 10.3201/eid2402.171268
- Nguyen, C. T., Le, N.-T., Tran, T. D.-H., Kim, E.-H., Park, S.-S., Luong, T. T., et al. (2014). *Streptococcus pneumoniae* ClpL modulates adherence to A549 human lung cells through Rap1/Rac1 activation. *Infect. Immun.* 82, 3802–3810. doi: 10.1128/IAI.02012-14
- Pan, Y. J., Fang, H. C., Yang, H. C., Lin, T. L., Hsieh, P. F., Tsai, F. C., et al. (2008). Capsular polysaccharide synthesis regions in *Klebsiella pneumoniae* serotype K57 and a new capsular serotype. *J. Clin. Microbiol.* 46, 2231–2240. doi: 10.1128/JCM.01716-07
- Pillai, D. R., Shahinas, D., Buzina, A., Pollock, R. A., Lau, R., Khairnar, K., et al. (2009). Genome-wide dissection of globally emergent multi-drug resistant serotype 19A *Streptococcus pneumoniae*. *BMC Genomics* 10:642. doi: 10.1186/1471-2164-10-642
- Plunkett, G. III, Rose, D. J., Durfee, T. J., and Blattner, F. R. (1999). Sequence of Shiga toxin 2 phage 933W from *Escherichia coli* O157:H7: shiga toxin as a phage late-gene product. *J. Bacteriol.* 181, 1767–1778.
- Prudhomme, M., Attaiech, L., Sanchez, G., Martin, B., and Claverys, J. P. (2006). Antibiotic stress induces genetic transformability in the human pathogen *Streptococcus pneumoniae*. *Science* 313, 89–92. doi: 10.1126/science.1127912
- Rabinovich, L., Sigal, N., Borovok, I., Nir-Paz, R., and Herskovits, A. A. (2012). Prophage excision activates *Listeria* competence genes that promote phagosomal escape and virulence. *Cell* 150, 792–802. doi: 10.1016/j.cell.2012.06.036
- Rohwer, F., and Edwards, R. (2002). The phage proteomic tree: a genome-based taxonomy for phage. *J. Bacteriol.* 184, 4529–4535. doi: 10.1128/JB.184.16.4529-4535.2002
- Scott, J., Nguyen, S. V., King, C. J., Hendrickson, C., and McShan, W. M. (2012). Phage-like *Streptococcus pyogenes* chromosomal islands (SpyCI) and mutator phenotypes: control by growth state and rescue by a SpyCI-encoded promoter. *Front. Microbiol.* 3:317. doi: 10.3389/fmicb.2012.00317
- Scott, J., Thompson-Mayberry, P., Lahmamsi, S., King, C. J., and McShan, W. M. (2008). Phage-associated mutator phenotype in group A streptococcus. *J. Bacteriol.* 190, 6290–6301. doi: 10.1128/JB.01569-07
- Shin, J., Baek, J. Y., Kim, S. H., Song, J. H., and Ko, K. S. (2011). Predominance of ST320 among *Streptococcus pneumoniae* serotype 19A isolates from 10 Asian countries. *J. Antimicrob. Chemother.* 66, 1001–1004. doi: 10.1093/jac/dkr048
- Singleton, R. J., Hennessy, T. W., Bulkow, L. R., Hammitt, L. L., Zulz, T., Hurlburt, D. A., et al. (2007). Invasive pneumococcal disease caused by nonvaccine serotypes among Alaska Native children with high levels of 7-valent pneumococcal conjugate vaccine coverage. *JAMA* 297, 1784–1792. doi: 10.1001/jama.297.16.1784
- Waldor, M. K. (1998). Bacteriophage biology and bacterial virulence. *Trends Microbiol.* 6, 295–297. doi: 10.1016/S0966-842X(98)01320-1
- Waldor, M. K., and Mekalanos, J. J. (1996). Lysogenic conversion by a filamentous phage encoding cholera toxin. *Science* 272, 1910–1914. doi: 10.1126/science.272.5270.1910

**Conflict of Interest Statement:** The authors declare that the research was conducted in the absence of any commercial or financial relationships that could be construed as a potential conflict of interest.

Copyright © 2019 Chen, Wang, Lin, Gong, Li, Huang and Hsieh. This is an open-access article distributed under the terms of the Creative Commons Attribution License (CC BY). The use, distribution or reproduction in other forums is permitted, provided the original author(s) and the copyright owner(s) are credited and that the original publication in this journal is cited, in accordance with accepted academic practice. No use, distribution or reproduction is permitted which does not comply with these terms.